

**Pattern Recognition and Tomographic  
Reconstruction with Terahertz Signals  
for Applications in Biomedical  
Engineering**

by

**Xiaoxia (Sunny) Yin**

Bachelor of Engineering (Industrial Electronics),  
Dalian University, 1996

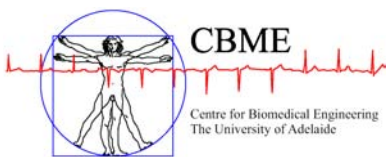
Thesis submitted for the degree of

**Doctor of Philosophy**

in

Electrical and Electronic Engineering  
University of Adelaide

2008



© 2008  
Xiaoxia (Sunny) Yin  
All Rights Reserved



— 尹晓霞 壬午年元月



壬午年元月

尹晓霞

Although the road ahead is endless and faraway,  
I still want to pursue and explore the truth in the world

—— Xiaoxia Yin writing on January 2009 (Personal Seal)

# Contents

|  |             |
|--|-------------|
| <b>Abstract</b>  | <b>xiii</b> |
| <b>Contents</b>  | <b>v</b>    |
| <b>Abstract</b>  | <b>xiii</b> |
| <b>Statement of Originality</b>                                | <b>xv</b>   |
| <b>Acknowledgments</b>   | <b>xvii</b> |
| <b>Conventions</b>   | <b>xix</b>  |
| <b>Publications</b>  | <b>xxi</b>  |
| <b>List of Figures</b>   | <b>xxv</b>  |
| <b>List of Tables</b>  | <b>xxxi</b> |
| <b>Chapter 1. Introduction and Motivation</b>                  | <b>1</b>    |
| 1.1 Introduction . . . . .                                     | 2           |
| 1.2 Background . . . . .                                       | 2           |
| 1.2.1 Terahertz radiation . . . . .                            | 2           |
| 1.2.2 THz pulsed imaging and continuous wave imaging . . . . . | 4           |
| 1.3 Outline of Thesis . . . . .                                | 4           |
| 1.4 Original contributions . . . . .                           | 6           |
| <b>Chapter 2. Terahertz Sources and Detectors</b>              | <b>11</b>   |
| 2.1 Introduction . . . . .                                     | 12          |
| 2.2 The history of T-rays . . . . .                            | 12          |
| 2.3 Laser sources . . . . .                                    | 15          |
| 2.3.1 Ti:sapphire-based lasers . . . . .                       | 15          |

|  |   |           |
|--|---|-----------|
| 2.3.2  | Free-electron lasers . . . . .                                    | 16        |
| 2.3.3  | Terahertz quantum cascade laser . . . . .                         | 18        |
| 2.4  | Terahertz semiconductor sources (THz Emitters) . . . . .          | 21        |
| 2.4.1  | Bulk electrooptic rectification (optical rectification) . . . . . | 22        |
| 2.4.2  | Ultra-fast charge transport . . . . .                             | 24        |
| 2.4.3  | Terahertz photomixing . . . . .                                   | 26        |
| 2.5  | Terahertz optical sampling techniques . . . . .                   | 27        |
| 2.5.1  | Coherent terahertz radiation detection . . . . .                  | 27        |
| 2.5.2  | Synchronous and asynchronous optical sampling . . . . .           | 29        |
| 2.6  | Chapter summary . . . . .   | 31        |
| <b>Chapter 3. Terahertz Imaging Modes</b>    |   | <b>33</b> |
| 3.1  | Three fundamental types of terahertz propagation . . . . .        | 34        |
| 3.1.1  | Transmission-type terahertz imaging . . . . .                     | 34        |
| 3.1.2  | Reflection-type terahertz imaging . . . . .                       | 36        |
| 3.2  | Terahertz imaging within diffraction-limit . . . . .              | 38        |
| 3.2.1  | Terahertz time-of-flight imaging . . . . .                        | 38        |
| 3.2.2  | Tomography with pulsed terahertz radiation . . . . .              | 39        |
| 3.2.3  | Terahertz continuous-wave imaging . . . . .                       | 44        |
| 3.3  | Terahertz imaging below the diffraction-limit . . . . .           | 49        |
| 3.4  | Chapter summary . . . . .   | 52        |
| <b>Chapter 4. Terahertz Imaging Analysis</b> |   | <b>53</b> |
| 4.1  | THz spectroscopy for biomedical signal identification . . . . .   | 54        |
| 4.1.1  | Time-resolved terahertz spectroscopy . . . . .                    | 54        |
| 4.1.2  | Frequency depend terahertz spectroscopy . . . . .                 | 55        |
| 4.1.3  | Time-frequency domain features of terahertz signals . . . . .     | 61        |
| 4.2  | 2D and 3D terahertz biomedical imaging . . . . .                  | 62        |
| 4.2.1  | Cancer cell detection . . . . .                                   | 63        |
| 4.2.2  | Brain section detection . . . . .                                 | 65        |
| 4.2.3  | Tablet coating detection . . . . .                                | 66        |

|  |  |            |
|--|--|------------|
| 4.3  | Pattern recognition of biomedical samples . . . . .  | 67         |
| 4.3.1  | Extracted parameters for terahertz pattern recognition . . . . .                           | 68         |
| 4.3.2  | Multispectral classification for terahertz pulsed imaging . . . . .                        | 69         |
| 4.3.3  | Classification of THz spectra in the wavelet domain . . . . .                              | 72         |
| 4.3.4  | Support vector machines for classification of the terahertz relevant frequencies . . . . . | 74         |
| 4.4  | Chapter summary . . . . .  | 74         |
| <b>Chapter 5. Pattern Formation and Recognition Using T-rays</b> |  | <b>75</b>  |
| 5.1  | Significance of a terahertz pattern recognition system . . . . .                           | 76         |
| 5.2  | Mode of the THz pattern recognition system . . . . .                                       | 77         |
| 5.3  | Configuration of the THz pattern recognition system . . . . .                              | 79         |
| 5.3.1  | Data acquisition using T-rays . . . . .  | 79         |
| 5.3.2  | Preprocessing . . . . .  | 80         |
| 5.3.3  | Representation of patterns for machine recognition . . . . .                               | 81         |
| 5.4  | Chapter summary . . . . .  | 82         |
| <b>Chapter 6. Wavelet Transforms</b>                             |  | <b>83</b>  |
| 6.1  | Wavelet and multiresolution processing . . . . .   | 84         |
| 6.2  | Wavelet transforms in one dimension . . . . .  | 89         |
| 6.2.1  | Wavelet series expansions and discrete wavelet transforms . . . . .                        | 89         |
| 6.2.2  | The fast wavelet transforms . . . . .  | 90         |
| 6.2.3  | Perfect reconstruction of 2-channel filter bank . . . . .                                  | 93         |
| 6.3  | Two dimensional discrete wavelet transforms . . . . .                                      | 95         |
| 6.4  | Discrete wavelet packet transforms . . . . .   | 96         |
| 6.5  | Wavelet denoising for THz-TDS pulses via the heuristic SURE threshold                      | 104        |
| 6.6  | Chapter summary . . . . .  | 107        |
| <b>Chapter 7. Feature Extraction and Selection</b>               |  | <b>109</b> |
| 7.1  | Role of feature selection and extraction . . . . .   | 110        |
| 7.2  | Feature extraction methods . . . . .   | 110        |
| 7.3  | Fourier transform for signal analysis . . . . .  | 112        |

7.4 AR and ARMA parametisation of wavelet coefficients . . . . . 113

7.4.1 AR model parameter estimation . . . . . 113

7.4.2 ARMA model parameter estimation . . . . . 114

7.4.3 Feature extraction via AR models over wavelet decomposition . . 115

7.5 System identification for feature extraction . . . . . 117

7.5.1 A subspace system identification algorithm . . . . . 118

7.5.2 Wavelet-packet identification of a system . . . . . 125

7.5.3 System identification via optimized Mertz apodization functions 132

7.6 Chapter summary . . . . . 134

**Chapter 8. Pattern Classification 137**

8.1 Mahalanobis distance . . . . . 138

8.1.1 Definition of Mahalanobis distance . . . . . 138

8.1.2 The Mahalanobis classifier via extracted features . . . . . 139

8.2 The Euclidean discrimination metric . . . . . 140

8.3 Overview of SVMs . . . . . 141

8.3.1 Binary classification of SVMs . . . . . 141

8.3.2 Pairwise SVM classification . . . . . 144

8.4 Classifier design . . . . . 145

8.4.1 Learning and adaption . . . . . 146

8.4.2 Evaluation . . . . . 146

8.4.3 Overfitting . . . . . 149

8.5 Chapter summary . . . . . 149

**Chapter 9. THz Pattern Recognition Experiments 151**

9.1 THz spectroscopy and imaging . . . . . 152

9.2 Enhanced T-ray signal classification using wavelet preprocessing . . . . 153

9.2.1 Feature extraction . . . . . 153

9.2.2 Classification . . . . . 154

9.2.3 Leave-one-out error estimator . . . . . 154

9.2.4 Results . . . . . 155



|  |  |            |
|--|--|------------|
| 9.2.5  | Conclusions . . . . .  | 159        |
| 9.3  | Classification using subspace and wavelet packet algorithms . . . . .                      | 159        |
| 9.3.1  | Evaluation of complex insertion loss, subspace and wavelet packet identification . . . . . | 160        |
| 9.3.2  | Signal processing assuming noisy background and sample response . . . . .                  | 163        |
| 9.3.3  | Evaluation via the discrimination metric . . . . .   | 166        |
| 9.3.4  | Conclusion . . . . .   | 169        |
| 9.4  | Application of AR models of wavelet sub-bands for classification . . . . .                 | 170        |
| 9.4.1  | Terahertz pulse measurements . . . . .   | 171        |
| 9.4.2  | Motivation . . . . .   | 172        |
| 9.4.3  | Resultant THz experiments . . . . .  | 174        |
| 9.4.4  | Conclusion and future work . . . . .   | 180        |
| 9.5  | Support vector machine applications in terahertz pulsed signal feature sets . . . . .      | 182        |
| 9.5.1  | Terahertz data representation . . . . .  | 183        |
| 9.5.2  | Terahertz feature extraction . . . . .   | 186        |
| 9.5.3  | Performance assessment of classification . . . . .   | 188        |
| 9.5.4  | The Fourier spectrum analysis . . . . .  | 189        |
| 9.5.5  | Resultant classification performance . . . . .   | 193        |
| 9.5.6  | Conclusion . . . . .   | 199        |
| 9.6  | Chapter summary . . . . .  | 200        |
| <b>Chapter 10. Terahertz Computed Tomography</b> |  | <b>203</b> |
| 10.1   | Brief review of THz imaging application . . . . .  | 204        |
| 10.2   | Methodology of computed tomography . . . . .   | 204        |
| 10.3   | Brief introduction to terahertz imaging for CT . . . . .                                   | 206        |
| 10.3.1   | Characteristics of diffraction grating pair . . . . .                                      | 208        |
| 10.4   | Calculation of terahertz parameters for reconstruction of THz CT . . . . .                 | 210        |
| 10.4.1   | Frequency domain sinogram for terahertz CT . . . . .                                       | 211        |
| 10.4.2   | Time domain sinogram for terahertz CT . . . . .  | 211        |
| 10.5   | Chapter summary . . . . .  | 213        |

|   |            |
|---|------------|
| <b>Chapter 11.2D Wavelet Segmentation in 3D T-ray CT</b>            | <b>215</b> |
| 11.1 An introduction for THz segmentation experiments . . . . .     | 216        |
| 11.2 Representation of a target sample . . . . .                    | 216        |
| 11.3 Wavelet based segmentation by fusion . . . . .                 | 217        |
| 11.3.1 Image fusion of T-ray CT images for a 3D target . . . . .    | 219        |
| 11.3.2 Discrete wavelet transforms in two dimensions . . . . .      | 219        |
| 11.3.3 2D wavelet scale correlation based segmentation . . . . .    | 220        |
| 11.4 Experimental result . . . . .                                  | 222        |
| 11.4.1 Extracted object segments . . . . .                          | 222        |
| 11.4.2 Segmentation quality . . . . .                               | 223        |
| 11.5 Chapter summary . . . . .                                      | 224        |
| <br>  |            |
| <b>Chapter 12.Wavelet-Based Terahertz Coherent Local Tomography</b> | <b>225</b> |
| 12.1 Motivation . . . . .   | 226        |
| 12.2 Two dimensional wavelet based CT reconstruction . . . . .      | 227        |
| 12.3 Local reconstruction using wavelets . . . . .                  | 230        |
| 12.3.1 Error analysis . . . . .                                     | 231        |
| 12.4 Implementation . . . . .                                       | 232        |
| 12.4.1 Experiments . . . . .  | 232        |
| 12.4.2 Algorithm summary . . . . .                                  | 239        |
| 12.5 Reconstruction results . . . . .                               | 240        |
| 12.5.1 Case study # 1: Polystyrene target . . . . .                 | 240        |
| 12.5.2 Case study # 2: Plastic vial target . . . . .                | 245        |
| 12.6 Future work . . . . .  | 245        |
| 12.7 Chapter summary . . . . .                                      | 247        |
| <br>  |            |
| <b>Chapter 13.Local CT Using a THz QCL</b>                          | <b>249</b> |
| 13.1 Introduction . . . . .   | 250        |
| 13.2 A T-ray quantum cascade laser . . . . .                        | 252        |
| 13.3 Implementation . . . . .                                       | 253        |
| 13.3.1 Experimental Considerations . . . . .                        | 253        |

|   |  |            |
|---|--|------------|
| 13.3.2  | Error analysis . . . . .   | 254        |
| 13.4  | Reconstruction Results . . . . .                                 | 262        |
| 13.4.1  | Slice One . . . . .  | 262        |
| 13.4.2  | Slice Two . . . . .  | 265        |
| 13.4.3  | Slice Three . . . . .  | 266        |
| 13.4.4  | Slice Four . . . . .   | 267        |
| 13.4.5  | Segment Evaluation . . . . .                                     | 267        |
| 13.5  | Chapter summary . . . . .  | 273        |
| <b>Chapter 14. Conclusions and Future Work</b>  |  | <b>275</b> |
| 14.1  | Introduction . . . . .   | 276        |
| 14.2  | Thesis summary . . . . .   | 276        |
| 14.2.1  | Summary of THz radiation and its sources and detectors . . . . . | 276        |
| 14.2.2  | Summary of THz imaging modes . . . . .                           | 277        |
| 14.2.3  | Summary of THz imaging analysis . . . . .                        | 277        |
| 14.2.4  | THz pattern recognition . . . . .                                | 278        |
| 14.2.5  | Wavelet and preprocessing . . . . .                              | 278        |
| 14.2.6  | Feature extraction and selection . . . . .                       | 279        |
| 14.2.7  | Pattern classification . . . . .                                 | 280        |
| 14.2.8  | THz pattern recognition experiments . . . . .                    | 280        |
| 14.2.9  | CT and THz CT . . . . .  | 282        |
| 14.2.10   | 2D wavelet-based segmentation by fusion in 3D THz CT . . . . .   | 282        |
| 14.2.11   | Wavelet-based terahertz coherent local tomography . . . . .      | 283        |
| 14.2.12   | Local computed tomography using a THz QCL . . . . .              | 283        |
| 14.3  | Future Directions . . . . .                                      | 284        |
| 14.3.1  | Curvelet transforms . . . . .                                    | 284        |
| 14.3.2  | Tomographic reconstruction . . . . .                             | 285        |
| 14.4  | Summary of original contributions . . . . .                      | 286        |
| 14.5  | In closing . . . . .   | 288        |
| <b>Appendix A. Oblique Projection Operation</b> |  | <b>289</b> |

|  |            |
|--|------------|
| <b>Appendix B. Back Projection Algorithms</b>                                  | <b>293</b> |
| B.1 Theory . . . . .   | 294        |
| <b>Appendix C. Error Analysis Regarding Wavelet Based Local Reconstruction</b> | <b>297</b> |
| C.1 Methodology . . . . .  | 298        |
| <b>Appendix D. Terahertz Imaging Systems</b>                                   | <b>303</b> |
| D.1 Ultrafast T-ray pulsed imaging . . . . .                                   | 304        |
| D.1.1 Ultrafast laser . . . . .  | 304        |
| D.1.2 Crossed-polariser detection . . . . .                                    | 304        |
| D.1.3 Hardware specifications . . . . .  | 304        |
| D.1.4 Software implementation . . . . .  | 305        |
| D.2 Continuous wave T-ray imaging via THz QCL . . . . .                        | 311        |
| D.2.1 THz QCL imaging . . . . .  | 311        |
| D.2.2 Hardware specifications . . . . .  | 312        |
| D.2.3 LabVIEW <sup>TM</sup> programming implement for data acquisition . . . . | 315        |
| <b>Appendix E. Matlab Code</b>   | <b>321</b> |
| E.1 Implemented Matlab toolboxes . . . . .                                     | 322        |
| E.2 Code listings . . . . .  | 322        |
| <b>Bibliography</b>  | <b>371</b> |
| <b>Glossary</b>  | <b>395</b> |
| <b>Index</b>   | <b>399</b> |
| <b>Résumé</b>  | <b>401</b> |
| <b>Scientific Genealogy</b>  | <b>403</b> |

# Abstract

Over the last ten years, terahertz (THz or T-ray) biomedical imaging has become a modality of interest due to its ability to simultaneously acquire both image and spectral information. Terahertz imaging systems are being commercialized, with increasing trials performed in a biomedical setting. Advanced digital image processing algorithms are greatly need to assist screening, diagnosis, and treatment. Pattern recognition algorithms play a critical role in the accurate and automatic process of detecting abnormalities when applied to biomedical imaging. This goal requires classification of meaningful physical contrast and identification of information in images, for example, distinguishing between different biological tissues or materials. T-ray tomographic imaging and detection technology contributes especially to our ability to discriminate opaque objects with clear boundaries and makes possible significant potential applications in both *in vivo* and *ex vivo* environments.

The Thesis consists of a number of Chapters, which can be grouped in to three parts. The first part provides a review of the state-of-the-art regarding THz sources and detectors, THz imaging modes, and THz imaging analysis. Pattern recognition forms the second part of this Thesis, which is represented via combining several basic operations: wavelet transforms and wavelet based signal filtering, feature extraction and selection, along with classification schemes for THz applications. Signal filtering in this Thesis is achieved via wavelet based de-noising. The ultrafast pulses generated terahertz time-domain spectroscopy (THz-TDS), which is demonstrated to justify their decomposition in the wavelet domain as it can provide better de-noising performance. Feature extraction and selection of the terahertz measurements rely on observed changes in pulse amplitude and phase, as well as scattering characteristics of several different types of powder samples under study. Additionally, three signal processing algorithms are adopted for the evaluation of the complex insertion loss function of such samples as lactose, mandelic acid, and dl-mandelic acid: (i) standard evaluation by ratioing the sample with the background spectra, (ii) a subspace identification algorithm, and (iii) a novel wavelet packet identification procedure. These system identification algorithms enable THz measurements to be transformed to features for THz pattern recognition. Meanwhile, a novel feature extraction method involving the use of Auto Regressive (AR) and Auto Regressive Moving Average (ARMA) models on the

wavelet transforms of measured T-ray pulse responses of *ex vivo* osteosarcoma cells as well as other biomedical materials is presented. Classification schemes are carried out via simple and robust schemes, such as the linear Mahalanobis distance classifier, and the non-linear Support Vector Machine (SVM) classifier. In particular, SVMs are used as a learning scheme to achieve the identification of two classes of RNA samples and multiple classes of powdered materials. Coherent terahertz detection hardware—THz time-domain spectroscopy (THz-TDS)—is used to obtain all the data for validation of these classification schemes.

The past decade has witnessed the tremendous development of terahertz instruments for detecting, storing, analysing, and displaying images. Terahertz time-domain spectroscopy (THz-TDS) is a broadband technique that generates and detects THz radiation in a synchronous and coherent manner. By contrast, the newly developed THz quantum cascade laser is a narrow-band radiation source that provides potential for realising compact systems; they produce image data with higher average power levels. The third part of this Thesis discusses methods to improve the capability of both broad- and narrow-band terahertz imaging, driven by computer-aided analytical techniques. A wavelet based reconstruction algorithm for terahertz computed tomography is represented to show how this algorithm can be used to rapidly reconstruct the region of interest (ROI) with a reduction in the measurements of terahertz responses, compared with a standard filtered back-projection technique. These reconstruction algorithms are applied to the analysis of acquired experimental data and to locally recover the two-dimensional (2D) and three-dimensional (3D) structures of several optically opaque objects. Moreover, a segmentation technique based on two dimensional wavelet transforms is investigated for the identification of different materials from the reconstructed CT image.

# Statement of Originality

This work contains no material that has been accepted for the award of any other degree or diploma in any university or other tertiary institution and, to the best of my knowledge and belief, contains no material previously published or written by another person, except where due reference has been made in the text.

I give consent to this copy of the thesis, when deposited in the University Library, being available for loan, photocopying, and dissemination through the library digital thesis collection, subject to the provisions of the Copyright Act 1968. Copying or publication or use of this thesis or parts thereof for financial gain is not allowed without the author's written permission. Due recognition shall be given the author, and the University of Adelaide, in any scholarly use that may be made of any material in the thesis.

31<sup>st</sup> December 2008

---

Signed

---

Date





# Acknowledgments

A great number of people have collaborated to make this PhD an exceptionally rewarding and memorable experience. I extend my sincerest thanks to my family, friends, colleagues, and supervisors for their support and encouragement.

I thank my supervisor Prof Derek Abbott for introducing me to the world of terahertz imaging and for the continuous flow of ideas that he provided. I also thank him for his encouragement and tireless work in reviewing journal publications and this Thesis. My co-supervisor Dr Brian W.-H. Ng provided welcome advice and contributed significantly to my PhD project. His work in proofing journal publications and this Thesis is also appreciated. Dr Samuel P. Mickan assisted in supervision in the early stages of this work and I would also like to thank him for his work.

I wish to thank Dr Bradley S. Ferguson (Tenix - Electronic Systems Division, now at Raytheon) for providing pulse CT data and Dr Bernd M. Fischer for providing the RNA data. Many thanks to Prof Sillas Hadjiloucas (Cybernetics, School of Systems Engineering, The University of Reading) for hosting my two month visit at Reading University and his important instruction in THz spectroscopy during this period. My thanks to Prof Lynn Gladden, (Head of Department of Chemical Engineering, University of Cambridge), and J. Axel Zeitler (Department of Chemistry, University of Cambridge) for their collaboration on the THz quantum cascade laser imaging work. In addition, I would like to express my appreciation to Prof Xi-Cheng Zhang, (J. Erik Jonsson Distinguished Professor, Director, Center for Terahertz Research at the Rensselaer Polytechnic Institute) for hosting my four month visit at Rensselaer Polytechnic Institute. His important support exposed me to an international advanced terahertz laboratory and a series of signal processing experiments.

Despite being so far away, my family in China and my friends in Adelaide have been a constant source of support. My very special appreciation goes to my husband, Cheng Shao, for being such a wonderful companion who brings so much happiness and love into my life.

Finally I am deeply grateful to the School of Electrical & Electronic Engineering at the University of Adelaide for the divisional scholarship that has allowed me to have this fantastic opportunity to live and work in Adelaide.

For personal financial support I would like to thank the Research Abroad Scholarship from The University of Adelaide (2006), the Roger Pysden Memorial Fellowship from the Australia Business, ABL State Chamber (2006), a Mutual Community Postgraduate Travel Grant from the University of Adelaide (2007), an Overseas Travel Fellowship from the Australian Research Council Nanotechnology Network (ARCNN) (2007), and a D. R. Stranks Travelling Fellowship from The University of Adelaide (2008).

Xiaoxia Yin, December 2008.

# Conventions

The following conventions have been adopted in this Thesis:

1. **Definitions.** The T-ray band is defined in this Thesis to span from 0.1 to 10 THz (THz =  $10^{12}$  Hz). This is an emerging definition in the literature. The T-ray band overlaps a little with the millimetre wave band (at lower T-ray frequencies) and the far-infrared band (at higher T-ray frequencies).

2. **Notation.** The acronyms and symbols used in this Thesis are defined in the Glossary on p. 403. Standard abbreviations are used for the order of magnitude: T, tera-,  $10^{12}$ ; G, giga-,  $10^9$ ; M, mega-,  $10^6$ ; k, kilo-,  $10^3$ ; m, milli-,  $10^{-3}$ ;  $\mu$ , micro-,  $10^{-6}$ ; n, nano-,  $10^{-9}$ ; p, pico-,  $10^{-12}$ ; f, femto-,  $10^{-15}$ .

3. **Units.** All T-ray electric field amplitude data in this Thesis is expressed in arbitrary units (AU). This means that the amplitude of the T-ray electric field has been normalised to a peak measurement, or to another reference measurement on the same system, depending on the experiment.

4. **Spelling.** Australian English spelling conventions have been used, as defined in the Macquarie English Dictionary (A. Delbridge (Ed.), Macquarie Library, North Ryde, NSW, Australia, 2001).

5. **Typesetting.** This document was compiled using LATEX2e.

6. **Mathematics.** MATLAB code was written using MATLAB Version 7.0. Manufacturer: the MathWorks Inc., Natick, MA, USA; URL: <http://www.mathworks.com>.

7. **Referencing.** The Harvard style has been adopted for referencing.

8. **Diagram colours.** The following colour scheme is approximately followed in the diagrams:

- Blue: T-ray beams (T-rays are invisible to the naked eye).
- Red: laser beams (the majority of laser beam sources appearing in the diagrams are from optical femtosecond lasers).
- Yellow: motion stages and samples (motion stages represent moving equipment, and samples can be composed of a wide variety of substances).

- Orange: electrooptic and semiconductor crystals (these are typically T-ray sources and detectors).
- Black/white: equipment, including optical components such as lenses and beam splitters.

9. **URLs.** Universal Resource Locators are provided in the Thesis for finding information on the world wide web using the hypertext transfer protocol (HTTP). The information at the locations listed was current on 31<sup>st</sup> December 2008.

# Publications

## Book Chapters

YIN-X. X, NG-B. W.-H, FERGUSON-B AND ABBOTT-D (2007). Wavelet based local coherent tomography with an application in terahertz imaging, in W. G. Kropatsch, M. Kampel, A. Hanbury (Eds.), *Computer Analysis of Images and Patterns, Lecture Notes in Computer Science*, Publ: Springer-Verlag, **4673**, pp. 878–885.

## Journal Articles

YIN-X. X, NG-B. W.-H, FERGUSON-B, AND ABBOTT-D (2008). Wavelet based local tomographic image reconstruction using terahertz techniques, *Digital Signal Processing*, DOI:10.1016/j.dsp.2008.06.009.

YIN-X. X, NG-B. W.-H, FERGUSON-B, MICKAN-S. P AND ABBOTT-D (2007). 2-D wavelet segmentation in 3-D T-ray tomography, *IEEE Sensors Journal*, **7**(3), pp. 342–343.

YIN-X. X, NG-B. W.-H, FISCHER-B.M, FERGUSON-B AND ABBOTT-D (2007). SVM applications in terahertz feature sets for identification of RNA data, *IEEE Sensors Journal*, **7**(11-12), pp. 1597–1608.

YIN-X. X, KONG-K. M., LIM-J. W., NG-B. W.-H, FISCHER-B. M, FERGUSON-B AND ABBOTT-D (2007). Enhanced T-ray signal classification using wavelet preprocessing, *Medical & Biological Engineering & Computing (Springer)*, **45**(6), pp. 611–616.

YIN-X. X, NG-B. W.-H, FERGUSON-B, HADJILOUCAS-S AND ABBOTT-D (2007). Application of auto-regressive models and wavelet sub-bands for classifying terahertz pulse measurements, *Journal of Biological Systems*, **15**(4), pp. 551–571.

WITHAYACHUMNANKUL-W, PNG-G, YIN-X. X, JONES-I, LIN-H, UNG-B, BALAKRISHNAN-J, NG-B. W.-H., FERGUSON-B, MICKAN-S. P AND ABBOTT-D (2007). T-ray sensing

and imaging, *Proceedings IEEE*, 95(8), pp. 1528–1558.

### Conference Articles

YIN-X. X, NG-B. W.-H., ZEITLER-J. A., NGUYEN-K. L., GLADDEN-L., AND ABBOTT-D. (2008). Local reconstruction for three dimensional terahertz imaging using a CW quantum cascade laser, *Proceedings of the 2008 International Conference on Image Processing, Computer Vision, & Pattern Recognition*, 14-17 July, 2008, Las Vegas, Nevada, USA, pp. 252–258. [Invited oral paper].

FISCHER-B. M., YIN-X. X, NG-B. W.-H., ABBOTT-D., GALVÕ-R. K. H., PAIVA-H. M., HADJILOUCAS-S., WALKER-G. C., AND BOWEN-J. W. (2008). Subspace and wavelet-packet algorithms for de-noising and classifying broadband THz transients, *33rd International Conference on Infrared, Millimeter, and Terahertz Waves (IRMMW-THz)*, 15-19 September, 2008, California Institute of Technology, Pasadena, California, USA, DOI:10.1109/ICIMW.2008.4665758.

YIN-X. X, HADJILOUCAS-S, FISCHER-B. M, PAIVA-H. M, GALVÕ-R. K. H, NG-B. W.-H, WALKER-G. C, BOWEN-J. W AND ABBOTT-D (2007). Classification of lactose and mandelic acid THz spectra using subspace and wavelet-packet algorithms, *Proceeding of SPIE Microelectronics, MEMS, and Nanotechnology*, 6798, Article Number 679814.

YIN-X. X, NG-B. W.-H, FERGUSON-B AND ABBOTT-D (2007). Terahertz local tomography using wavelets, *IEEE Joint 32nd International Conference on Infrared and Millimeter Waves and 15th International Conference on Terahertz Electronics (IRMMW-THz 2007)*, 2-5 September, 2007, Cardiff, UK, pp. 514–515.

YIN-X. X, NG-B. W.-H, FERGUSON-B, MICKAN-S. P AND ABBOTT-D (2007). 2D wavelet-based segmentation by fusion in 3D terahertz tomography, *IEEE International Symposium on Industrial Electronics (ISIE)*, 4-7 June, 2007, Vigo, Spain, pp. 3409-3414. [This paper won an IEEE (ISIE) student best paper].

YIN-X. X, NG-B. W.-H, FERGUSON-B, MICKAN-S. P AND ABBOTT-D (2006). Feature extraction from terahertz pulses for classification of RNA data via support vector machines, *Proceeding of SPIE Micro- and Nanotechnology: Materials, Processes,*

---

*Packaging, and Systems III*, 11-13 December 2006, Adelaide, Australia, **6415**, Article Number 641516.

YIN-X. X, NG-B. W.-H, FERGUSON-B, MICKAN-S.P AND ABBOTT-D (2006). Wavelet based segment detection and feature extraction for 3D T-ray CT pattern classification, *IEEE Signal Processing Society: 12th Digital Signal Processing Workshop 4th signal Processing Education Workshop: Filtering*, September 24-27, 2006, Wyoming, USA, pp. 602–607.

YIN-X. X, NG-B. W.-H, FERGUSON-B, MICKAN-S. P AND ABBOTT-D (2006). Information fusion and wavelet based segment detection with applications to the identification of 3D target T-ray CT imaging, *IEEE Joint 31st International Conference on Infrared and Millimeter Waves and 14th International Conference on Terahertz Electronics (IRMMW-THz 2006): Biological and Medical Applications*, September 18-22, 2006, Shanghai, China, p. 187.

YIN-X. X, NG-B. W.-H, FERGUSON-B, MICKAN-S. P AND ABBOTT-D (2006). Statistical model for the classification of the wavelet transforms of T-ray pulses, *IEEE International Conference on Pattern Recognition (ICPR 2006): Advances in Basic Methodology II*, 20-24 August 2006, Hong Kong, China, **III**, pp. 236–239. [This paper won The International Association for Pattern Recognition (IAPR) Hong Kong travel stipend].

YIN-X. X, NG-B. W.-H, FERGUSON-B, MICKAN-S. P AND ABBOTT-D (2006). Classification of human osteosarcoma cells via wavelet transform, and AR parametric modeling of T-ray pulsed signals, *Wavelets and Applications Conference (WavE 2006)*, July 10-14 2006, Lausanne, Switzerland, p. A-80. [This paper won a WavE Swiss travel fellowship].

YIN-X. X, NG-B. W.-H, FERGUSON-B, MICKAN-S. P AND ABBOTT-D (2005). One dimensional wavelet transforms and their application to T-ray pulsed signal identification, *Proceeding of SPIE Photonics: Design, Technology and Packaging II*, December 11-15, 2005, Brisbane, Australia, **6038**, Article Number 603829.





# List of Figures

|       |  |    |
|-------|--|----|
| 1.1   | Electromagnetic spectrum . . . . .   | 3  |
| 1.2   | Thesis structural flow chart . . . . .   | 7  |
| <hr/> |  |    |
| 2.1   | Ti:sapphire-based lasers . . . . .   | 17 |
| 2.2   | A schematic of a THz free-electron laser . . . . .                               | 18 |
| 2.3   | Schematic diagrams of terahertz BTC quantum cascade laser designs . . . . .      | 20 |
| 2.4   | Two-colour terahertz quantum cascade laser spectrum . . . . .                    | 21 |
| 2.5   | Optical rectification and ultra-fast charge transport schemes . . . . .          | 23 |
| 2.6   | Magnetic-field-enhanced generation of T-rays in semiconductor surfaces . . . . . | 25 |
| 2.7   | Photomixing schematics . . . . .   | 27 |
| 2.8   | Sketch of an electrooptic sampling setup . . . . .                               | 28 |
| 2.9   | Sketch of a PCA used for photoconductive sampling . . . . .                      | 29 |
| 2.10  | Pump-probe delay stage . . . . .   | 30 |
| <hr/> |  |    |
| 3.1   | Transmission mode THz imaging . . . . .  | 35 |
| 3.2   | Reflection mode THz imaging . . . . .  | 37 |
| 3.3   | Time-of-flight imaging . . . . .   | 39 |
| 3.4   | Single-cycle THz tomography . . . . .  | 40 |
| 3.5   | Terahertz multistatic reflection imaging . . . . .                               | 41 |
| 3.6   | Terahertz holography . . . . .   | 42 |
| 3.7   | Holographic imaging reconstruction . . . . .                                     | 43 |
| 3.8   | Synthetic aperture radar algorithms using T-rays . . . . .                       | 45 |
| 3.9   | All-optoelectronic continuous wave THz imaging . . . . .                         | 46 |
| 3.10  | THz QCL imaging at a standoff distance . . . . .                                 | 48 |
| 3.11  | Near-field (NF) imaging . . . . .  | 50 |
| 3.12  | THz near-field imaging employing synchrotron radiation . . . . .                 | 51 |

---

|      |  |    |
|------|--|----|
| 4.1  | Water molecule vibrational moles . . . . .                                     | 56 |
| 4.2  | Retinal isomer . . . . .   | 60 |
| 4.3  | Time-frequency domain features of THz signals . . . . .                        | 61 |
| 4.4  | Pulsed THz imaging of a human tooth and a sample of pork . . . . .             | 63 |
| 4.5  | Skin cancer THz detection . . . . .  | 64 |
| 4.6  | Breast cancer THz inspection . . . . .   | 65 |
| 4.7  | Rat brain image using a THz QCL . . . . .                                      | 66 |
| 4.8  | Thickness measurements of soft gelatin capsules using THz 3D imaging . . . . . | 67 |
| 4.9  | Multispectral clustering for THz classification . . . . .                      | 70 |
| 4.10 | Principal component analysis of THz spectral . . . . .                         | 72 |
| 4.11 | Optimal THz classification in the wavelet domain . . . . .                     | 73 |

---

|     |   |    |
|-----|---|----|
| 5.1 | Pattern recognition of chicken and beef . . . . . | 78 |
| 5.2 | THz scanner and data recognition system . . . . . | 79 |

---

|     |   |     |
|-----|---|-----|
| 6.1 | Block diagram for the analysis and synthesis stages of the Fast Wavelet Transform (FWT) . . . . . | 90  |
| 6.2 | Fast Wavelet Transforms . . . . .   | 92  |
| 6.3 | Time-frequency boxes of two wavelets $\psi_{j,k}$ and $\psi_{J_0,K_0}$ . . . . .                  | 92  |
| 6.4 | Illustration of the 2D discrete wavelet transform procedure . . . . .                             | 97  |
| 6.5 | The procedure of discrete wavelet packet transform . . . . .                                      | 98  |
| 6.6 | The procedure of discrete wavelet packet transform . . . . .                                      | 101 |
| 6.7 | A quick searching of the best bases . . . . .   | 103 |

---

|     |  |     |
|-----|--|-----|
| 7.1 | Illustration of the $DC^{ARMA}$ feature matrix calculated over three levels of wavelet decomposition . . . . . | 117 |
| 7.2 | Block diagrams of noisy state-space models . . . . .   | 124 |
| 7.3 | Wavelet-packet model structure . . . . .   | 127 |

---

|       |   |     |
|-------|---|-----|
| 7.4   | Model identification of a sample response for a given frequency sub-band                      | 128 |
| 7.5   | The Choice of the best decomposition tree . . . . .   | 131 |
| 7.6   | Plots of Mertz asymmetric triangular windows on the measured THz signals . . . . .            | 134 |
| ————— |   |     |
| 8.1   | A schematic of the Mahalanobis distance classifier . . . . .                                  | 139 |
| 8.2   | Illustration of the procedure for pairwise classification . . . . .                           | 145 |
| 8.3   | Design of a classifier . . . . .  | 147 |
| ————— |   |     |
| 9.1   | Illustration of a femtosecond laser-based T-ray functional imaging system                     | 152 |
| 9.2   | Measured time domain T-ray signals and phase spectrum . . . . .                               | 155 |
| 9.3   | Amplitude scatter plot . . . . .  | 159 |
| 9.4   | THz measurements of a lactose sample . . . . .  | 162 |
| 9.5   | Subspace identification of lactose responses . . . . .  | 163 |
| 9.6   | Wavelet-packet identification of lactose responses . . . . .                                  | 164 |
| 9.7   | Degradation of lactose responses . . . . .  | 165 |
| 9.8   | Subspace identification of noisy lactose responses . . . . .                                  | 166 |
| 9.9   | Wavelet-packet identification of noisy lactose responses . . . . .                            | 167 |
| 9.10  | Wavelet-packet identification of lactose responses with different noise levels . . . . .      | 168 |
| 9.11  | Plots of resultant discrimination metric . . . . .  | 169 |
| 9.12  | Comparisons of the time domain signals for NHB and HOS cells . . . . .                        | 175 |
| 9.13  | Illustration of the current classification algorithm . . . . .                                | 176 |
| 9.14  | Scatter plots of learning vectors . . . . .   | 179 |
| 9.15  | Chemical structure of RNA samples . . . . .   | 184 |
| 9.16  | T-ray transmission image of poly-A and poly-C RNA samples on a biochip substrate . . . . .    | 186 |
| 9.17  | Photo of a teflon sample holder for measurement fixed thickness of powdered samples . . . . . | 187 |
| 9.18  | Illustration of T-ray spectra of RNA . . . . .  | 190 |

|       |   |     |
|-------|---|-----|
| 9.19  | An illustration of binary classification for the recognition of RNA samples   | 191 |
| 9.20  | Illustration of Fourier spectrum . . . . .  | 192 |
| 9.21  | Plot of learning vector pattern . . . . .   | 193 |
| 9.22  | Learning vectors for the six-class examples are plotted . . . . .   | 194 |
| 9.23  | Plots of classification accuracy regarding RNA samples . . . . .  | 195 |
| 9.24  | Illustration regarding the variation with respect to the number of SVs<br>and classification accuracy . . . . .   | 196 |
| <hr/> |   |     |
| 10.1  | Illustration of general scheme for computed tomography . . . . .  | 206 |
| 10.2  | A chirped probe pulse terahertz imaging system . . . . .  | 207 |
| 10.3  | Schematic of THz CT sampling and the relative coordinate systems . . .  | 208 |
| 10.4  | The geometry of a diffraction grating for chirped pulsed compression.<br>The grating is used to impart a linear chirp to a laser pulse. The mirror<br>M reflects the beam back into the grating pair. The optical path length is<br>greater for longer wavelengths. The angle of incidence is $\gamma$ and $\theta$ is the<br>angle between incident and diffracted rays. . . . . | 209 |
| 10.5  | A cross-correlation algorithm . . . . .   | 213 |
| <hr/> |   |     |
| 11.1  | A nested structure for the illustration of T-ray CT system . . . . .  | 217 |
| 11.2  | Illustration of the reconstructed T-ray CT slices . . . . .   | 218 |
| 11.3  | Illustration of T-ray signals and spectra . . . . .   | 218 |
| 11.4  | Illustration of reconstructed central slice T-ray CT images . . . . .   | 220 |
| 11.5  | Illustration of the sub-images via reconstructed approximation coefficients   | 220 |
| 11.6  | Segmented images at different heights . . . . .   | 222 |
| 11.7  | Illustration of the centroid locations of the target tube segment . . . . .   | 223 |
| <hr/> |   |     |
| 12.1  | Wavelet ramp filters . . . . .  | 228 |
| 12.2  | Target object photographs . . . . .   | 233 |
| 12.3  | Wavelet based ramp filtered projections with extrapolation . . . . .  | 236 |
| 12.4  | Projection in the off-center area . . . . .   | 237 |

|       |   |     |
|-------|---|-----|
| 12.5  | Wavelet based ramp filtered projections after applying a shape scaling factor of 1/3 . . . . .        | 238 |
| 12.6  | Wavelet and scaling ramp filtering of sinograms towards the polystyrene target . . . . .              | 241 |
| 12.7  | Reconstruction results of the polystyrene target with 46% of full data at centered area . . . . .     | 242 |
| 12.8  | Reconstruction results of the polystyrene target with 33% of full data at off-centered area . . . . . | 244 |
| 12.9  | Reconstruction results of a vial slice from the nested structure . . . . .                            | 246 |
| <hr/> |   |     |
| 13.1  | Terahertz quantum cascade laser setup . . . . .   | 252 |
| 13.2  | Photographs and image reconstruction of a clown's head with a hole inside . . . . .                   | 254 |
| 13.3  | Illustration of a typical local reconstruction . . . . .  | 255 |
| 13.4  | Segmented image via fuzzy <i>c</i> -means thresholding . . . . .                                      | 256 |
| 13.5  | A cropped sinogram image . . . . .  | 257 |
| 13.6  | Resultant local reconstructions at Slice 1 . . . . .  | 259 |
| 13.7  | Plot of the measured ground truth . . . . .   | 260 |
| 13.8  | Resultant segments and differences at Slice 1 . . . . .   | 261 |
| 13.9  | Resultant local reconstructions at Slice 2 . . . . .  | 263 |
| 13.10 | Resultant segments and the differences at Slice 2 . . . . .   | 264 |
| 13.11 | Resultant local reconstructions at Slice 3 . . . . .  | 266 |
| 13.12 | Resultant segments and the differences at Slice 3 . . . . .   | 268 |
| 13.13 | Resultant local reconstructions at Slice 4 . . . . .  | 269 |
| 13.14 | Resultant segments and the differences at Slice 4. . . . .  | 270 |
| <hr/> |   |     |
| A.1   | Schematic of oblique projection . . . . .   | 290 |
| A.2   | The projections regarding state-space sequences . . . . .   | 291 |
| <hr/> |   |     |
| <hr/> |   |     |

---

|      |  |     |
|------|--|-----|
| D.1  | Photograph of an ultrafast laser . . . . .   | 305 |
| D.2  | Photograph of crossed polarisers in electrooptic sampling . . . . .  | 306 |
| D.3  | Schematic of the femtosecond laser-based T-ray chirped functional imaging system based on a pump-probe configuration . . . . . | 307 |
| D.4  | Screen shots of the MFCPentamax software and the Labview tomography application . . . . .                                      | 308 |
| D.5  | Screen shot of control software for operating T-ray TDS experiments via a Picometrix system . . . . .                          | 310 |
| D.6  | Experimental apparatus for a terahertz QCL imaging system that is used to realise terahertz CT imaging . . . . .               | 312 |
| D.7  | Photographs of an THz QCL and its experiment setup for THz CW imaging . . . . .  | 313 |
| D.8  | Photograph of right part of the experimental apparatus shown in Fig. D.6   | 314 |
| D.9  | Mapping the QCL beam shape . . . . .   | 315 |
| D.10 | Screen shots of LabVIEW <sup>TM</sup> programme to control motion stages via motion controllers . . . . .                      | 318 |
| D.11 | Screen shots of LabVIEW <sup>TM</sup> programme to control rotation stages via motor controllers . . . . .                     | 319 |

---

# List of Tables

|      |   |     |
|------|---|-----|
| 7.1  | Standard approaches in pattern recognition . . . . .  | 111 |
| 9.1  | The classification accuracies for the seven types of powder samples . . .   | 157 |
| 9.2  | The calculated squared error variances on cell samples . . . . .  | 177 |
| 9.3  | Percentage classification accuracy of T-ray pulses travelling through cell samples . . . . .  | 178 |
| 9.4  | The calculated squared error variances on powder samples . . . . .  | 179 |
| 9.5  | Squared error variances of ARMA on powder samples . . . . .   | 180 |
| 9.6  | Percentage classification accuracy of several powder samples . . . . .  | 180 |
| 9.7  | Percentage classification accuracy of several powder samples . . . . .  | 180 |
| 9.8  | Percentage Classification accuracy of several powder samples . . . . .  | 181 |
| 9.9  | Varying penalty parameter $C$ and the polynomial kernel $p=1$ are implemented for the parameter calculation regarding SVMs . . . . .  | 197 |
| 9.10 | Varying penalty parameter $C$ and the polynomial kernel $p=2$ are implemented for the parameter calculation regarding SVMs . . . . .  | 197 |
| 9.11 | Varying penalty parameter $C$ and the polynomial kernel $p=3$ are implemented for the parameter calculation regarding SVMs . . . . .  | 198 |
| 13.1 | Table of the radii of the ROE and ROI . . . . .   | 269 |
| 13.2 | Illustration of the centroid coordinates . . . . .  | 271 |
| 13.3 | Illustration of error ratio . . . . .   | 272 |
| D.1  | The description regarding the full system layout components, along with the hardware specifications shown in Fig. D.3. . . . .  | 309 |
| D.2  | The description regarding the full system layout components, shown in Fig. D.3, including a detailed description of the role these components play in the system, and the manufacturers. The numbers correspond to the items listed in Table D.1. . . . . | 311 |
| D.3  | Summary of electronic components of the THz QCL imaging system . .  | 316 |